

## In-Situ X-Ray Diffraction Study of Metal Hydride Formation in Palladium and Palladium-Based Alloy Electrodes under Cathodic Hydrogen Charging

Ken-ichi MACHIDA† and Michio ENYO\*

Research Institute for Catalysis, Hokkaido University, Sapporo 060

(Received September 28, 1988)

An in situ X-ray diffraction (XRD) technique reported earlier was improved and employed to study the hydride formation in Pd and Pd–Au alloy foils and amorphous Pd–Zr alloy ribbons during cathodic hydrogen charging or its reverse process. The phase transformation from  $\alpha$ - to  $\beta$ -PdH<sub>x</sub> in the Pd electrode, accompanied by an increase in the cell volume, was demonstrated to take place by the formation of a  $\beta$  phase domain in the bulk during the cathodization. The lattice constant was discontinuously changed from  $a \approx 3.92$  to  $4.04$  Å and such a discontinuous change was observed on the Pd<sub>90</sub>Au<sub>10</sub> alloy as well. However, no phase transformation was observed on the Pd–Au alloys with the Pd content of 70 at.% or below, where the lattice constant increased continuously with an increase in the negative potential for the cathodic polarization. No crystallization in the amorphous Pd–Zr alloy ribbon electrodes was detected after hydrogen charging.

Electrochemical oxidation/reduction reactions are often accompanied by the occlusion of electrolysis products into the electrode, which may cause a phase transformation or formation of other phases. A typical example is the hydride formation due to hydrogen absorption into electrodes of some metals or alloys.<sup>1)</sup> An X-ray diffraction (XRD) technique may be used to detect such changes. A set of ex situ XRD measurements on a relationship between the  $\alpha$  and  $\beta$  phases of Pd and its alloys has demonstrated that the phase transformation proceeds even electrochemically and also is modified by the alloying element and its content.<sup>2–4)</sup> However, the measurements should preferably be made in situ, as the new phases formed may be unstable when the electrodes are taken out of the system in which the electrochemical environment has been controlled.

Uno Falk et al.<sup>5)</sup> have reported, by using an in situ XRD technique, clear phase changes during charging and discharging of Cd, Fe, or Ni electrode in Jungner and Edison secondary cells. Recently, Nazri and Müller<sup>6)</sup> have applied this technique to a Li electrode in nonaqueous solutions. The present authors also have reported the phase transformation accompanied by the hydride formation in Pd electrodes.<sup>7)</sup> In this work, the in situ XRD technique is improved for accepting samples with low crystallinity and applied to the study of hydride formation in Pd, Pd–Au, and amorphous Pd–Zr alloy electrodes as a function of the cathodization conditions.

### Basic Relations in Hydrogen Electrode Reaction.

The hydrogen electrode reaction on Pd, Pd–Au, or amorphous Pd–Zr alloy electrodes has been shown to proceed via the Volmer–Tafel reaction scheme.<sup>8–10)</sup> In this mechanism, the equivalent hydrogen pressure  $\bar{P}_{H_2}$  during the polarization as referred to its value  $\bar{P}_{H_2, o}$  at equilibrium potential is related to the overpotential component  $\eta'_2$  for the Tafel step,  $2H(ads) \rightarrow H_2$ , by the

relation,<sup>8)</sup>

$$-\eta'_2 = (RT/2F) \ln(\bar{P}_{H_2}/\bar{P}_{H_2, o}) \quad (1)$$

This overpotential component can readily be evaluated from electrode potential-time transient curves.<sup>8)</sup> Although this relation has been substantiated by various analyses, a direct demonstration under an in situ condition is desirable. The in situ XRD analysis by monitoring the  $\eta'_2$  may be expected to give conclusive information about the metal hydride phase relation in hydrogen absorbing metal or alloy electrodes under cathodic polarization.

### Experimental

**Electrodes.** The test electrodes used were Pd foil and Pd<sub>100-x</sub>Au<sub>x</sub> ( $x=10, 30, 45$ , and  $60$ ) alloy foils of  $10 \times 10$  mm in size and  $12.5$  or  $50$   $\mu$ m in thickness which were spot-welded to Ta wires sealed beforehand into glass tubings. Similarly, an amorphous Pd<sub>35</sub>Zr<sub>65</sub> ribbon ( $0.8$  mm wide and ca.  $20$   $\mu$ m in thickness) was cut to pieces of  $10$  mm long, which were spot-welded on a Ta net of  $10 \times 10$  mm, followed by etching in dilute HF solution for several ten seconds in order to remove a catalytically inactive ZrO<sub>2</sub> surface layer.

**Apparatus and Method.** A syringe-type electrochemical cell<sup>11)</sup> consisting of the working electrode, a Pt net counter electrode, a Ag/AgCl reference electrode, and a window of Kapton foil (polyimide sheet) for X-ray observations<sup>7)</sup> was used (Fig. 1). In order to make the cell applicable to samples of low crystallinity (e.g. oxides or, particularly, amorphous-like samples), a modification was introduced to minimize the background signal from the Kapton foil window, especially in a low  $2\theta$  angle region, in such a way that X-ray beams passed vertically through the window over the whole scan angle. The glass cell was mounted on a Rigaku  $\theta$ – $\theta$  scan goniometer which had a fixed and horizontal sample stage, rotatable X-ray source and a detector. The X-ray radiation used was Mo  $K\alpha$  ( $\lambda=0.71069$  Å) monochromatized with a graphite plate. All the electrochemical measurements were carried out at room temperature (about  $293$  K) in  $0.5$  M H<sub>2</sub>SO<sub>4</sub> ( $M=\text{mol dm}^{-3}$ ) under H<sub>2</sub> atmosphere. The XRD data obtained were calibrated by using silicon powder comounted with epoxy resin on the electrode. All potentials were

† Present address: Department of Applied Chemistry, Faculty of Engineering, Hokkaido University, Sapporo 060.



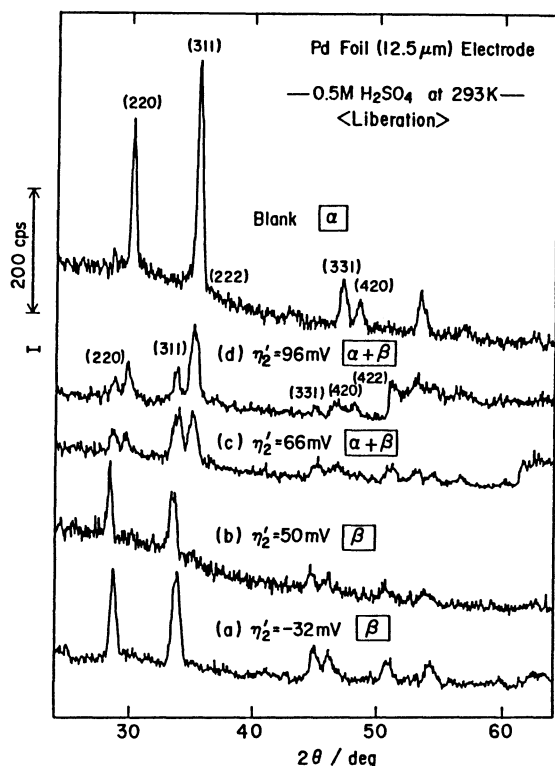


Fig. 3. In situ XRD patterns observed on a Pd foil electrode at various  $\eta_2'$  values during the hydrogen liberation hemicycle. Polarization time was 0.5 h for  $\eta_2' = -32$  mV or 3 h for  $\eta_2' = 50, 66$ , and 96 mV. 0.5M  $H_2SO_4$ .

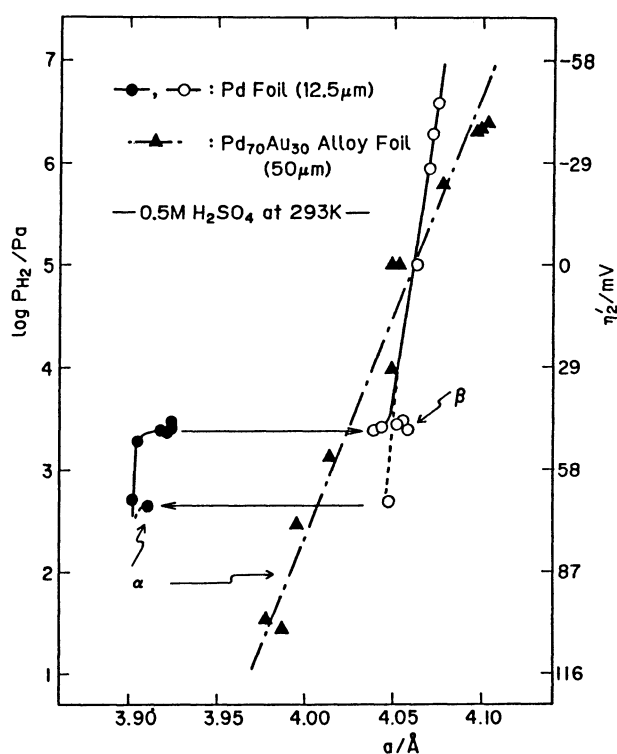


Fig. 4. Relationships between the  $\eta_2'$  (or  $\bar{P}_{H_2}$ ) and lattice constant observed for  $\alpha$  and  $\beta$  phases on the Pd-H and Pd<sub>70</sub>Au<sub>30</sub>-H systems.

under the condition in which electrode potential was shifted stepwise to more positive potentials up to  $\eta_2' = 96$  mV (a hydrogen liberation hemicycle). The  $\beta$  phase in the Pd foil electrode was kept even under the polarization of  $\eta_2' = 50$  mV, but it was partly retransformed to  $\alpha$  phase at  $\eta_2' = 66$  mV, giving the XRD signal originated from  $\alpha$  phase which has a comparable intensity with  $\beta$  phase. The amount of  $\alpha$  phase increased with increase of the potential for polarization, viz.  $\eta_2' = 96$  mV. On the other hand, no retransformation to  $\alpha$  phase was observed at the potential in the  $\alpha$ - $\beta$  transformation region during the hydrogen absorption hemicycle ( $\eta_2' = 50$  mV), even after a longer

Table 1. Lattice Constants for a Series of Pd<sub>100-x</sub>Au<sub>x</sub> Alloy Foils before and after Cathodic Polarization (in 0.5 M  $H_2SO_4$ )

Alloy	Lattice constant/Å	
	before	after <sup>a)</sup>
Pd <sub>90</sub> Au <sub>10</sub>	3.90	4.07
Pd <sub>70</sub> Au <sub>30</sub>	3.93	4.05
Pd <sub>55</sub> Au <sub>45</sub>	3.95	4.04
Pd <sub>40</sub> Au <sub>60</sub>	3.97	4.03

a) Cathodization potential  $\eta_2' = ca. -5$  mV.

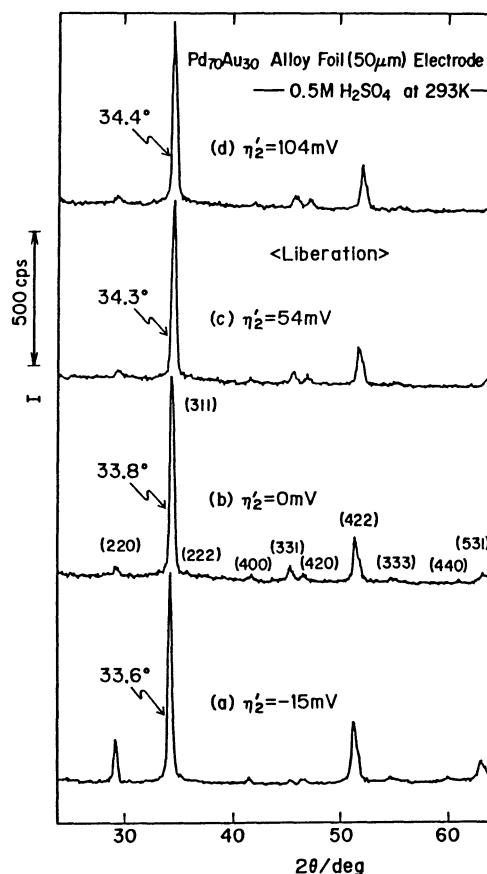


Fig. 5. In situ XRD patterns observed on a Pd<sub>70</sub>Au<sub>30</sub> alloy foil electrode at various  $\eta_2'$  values during the hydrogen liberation hemicycle. Polarization time was 0.5 h. 0.5 M  $H_2SO_4$ .

polarization period, e.g. 20 h.

The relationship between the  $\eta'_2$  (or  $\bar{P}_{H_2}$ ) and lattice constant observed on the Pd foil are shown in Fig. 4. A clear hysteresis is seen on the hydrogen pressure versus hydrogen content curves between the hydrogen liberation and absorption hemicycles. Such a hysteresis well corresponds to that observed in the hydrogen charging-discharging cycle in gaseous  $H_2$ ,<sup>12)</sup> with the extent dependent on the duration of the polarization.

**Pd-Au Alloy Foil Electrodes.** The lattice constants of a series of Pd-Au alloy electrodes before and after the polarization at  $\eta'_2 \approx -5$  mV are summarized in Table 1. The increase of the Au content in the Pd-Au alloys resulted in an enlargement of the lattice constants (see data in Table 1), while the inverse tendency was observed after the cathodic polarization. This indicates that the Pd-Au alloys become difficult to absorb hydrogen with an increase in the Au content. This observation agrees with results obtained on Pd alloyed with Au<sup>3)</sup> or the other group IB metals.<sup>4)</sup>

In Fig. 5, the in situ XRD patterns obtained on the Pd<sub>70</sub>Au<sub>30</sub> electrode in the hydrogen liberation hemicycle are shown. There was no discontinuous change in the lattice constant obtained at various  $\eta'_2$  values and, instead, the  $2\theta$  value of (311) reflection from the  $\alpha$  phase changed continuously from 33.6 to 34.4° as indicated in the figure, which gave the lattice constant of 3.986–4.078 Å. In this way, the  $\alpha$ - $\beta$  phase transformation such as that observed on Pd foils did not take

place in the Pd<sub>70</sub>Au<sub>30</sub> alloy foil electrode. This result is in good agreement with similar characters observed in the case of absorption of hydrogen into Pd-Au alloys.<sup>3)</sup>

**Amorphous Pd<sub>35</sub>Zr<sub>65</sub> Alloy Ribbon Electrodes.** Figure 6 shows in situ XRD patterns observed on amorphous Pd<sub>35</sub>Zr<sub>65</sub> alloy ribbon electrodes before and after the etching treatment in dilute HF solution. Both the untreated and HF-treated specimens before the polarization gave no peak in the XRD patterns originating from crystalline phases (see blank one). Further, no XRD peak corresponding to hydrides was detected even under the cathodic polarization conditions ( $\eta'_2 = \text{ca. } -30$  mV). This result may be important in suggesting that the amorphous alloy materials are not likely to encounter hydrogen embrittlement due to recrystallization even under strong hydrogen charging conditions such as the one in the electrochemical cathodic polarization, and thus they may be used in hydrogen storage-type batteries.

### Conclusion

An in situ XRD technique was developed and applied to the studies of phase changes during metal hydride formation in Pd and Pd-Au alloy foil and amorphous Pd-Zr ribbon electrodes. The technique may be applicable to studies of composition or structure changes in other electrochemical processes. The  $\alpha$ - $\beta$  phase transformation in PdH<sub>x</sub> or no such phase changes in Au-rich Pd-Au alloy foils and amorphous Pd-Zr alloy ribbons were indicated.

The present work has been partly supported by Grants-in-Aid for Scientific Research from the Ministry of Education, Science and Culture.

### References

- 1) "Hydrogen for Energy Storage," ed by A. F. Andresen and A. J. Maeland, Pergamon Press, New York (1978), p. 19.
- 2) F. A. Lewis, "The Palladium Hydrogen System," Academic Press, New York (1967), pp. 70–93.
- 3) A. Maeland and T. B. Flanagan, *J. Phys. Chem.*, **69**, 3575 (1965).
- 4) A. W. Carson and F. A. Lewis, *Trans. Faraday Soc.*, **63**, 1453 (1967); R. Burch and R. G. Buss, *J. Chem. Soc., Faraday Trans. 1*, **71**, 913 (1975).
- 5) S. Uno Falk, *J. Electrochem. Soc.*, **107**, 661 (1960); A. J. Salkind, C. J. Venuto, and S. Uno Falk, *ibid.*, **111**, 493 (1964).
- 6) G. Nazri and R. H. Müller, *J. Electrochem. Soc.*, **132**, 1385, 2051, 2054 (1985).
- 7) K. Machida and M. Enyo, *Chem. Lett.*, **1986**, 1437.
- 8) T. Maoka and M. Enyo, *Electrochim. Acta*, **26**, 607, 615 (1981).
- 9) M. Enyo, *J. Res. Inst. Catal., Hokkaido Univ.*, **30**, 11 (1982).
- 10) M. Enyo, T. Yamazaki, K. Kai, and K. Suzuki, *Electrochim. Acta*, **28**, 1573 (1983).
- 11) K. Kunitatsu, *Hyomen (Surface)*, **20**, 197 (1982).
- 12) Ref. 2, p. 33.

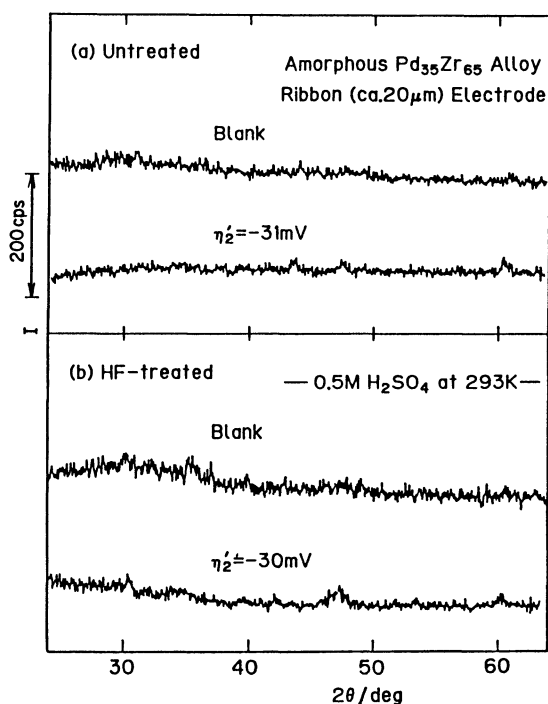


Fig. 6. In situ XRD patterns observed on an amorphous Pd<sub>35</sub>Zr<sub>65</sub> ribbon electrode at various  $\eta'_2$  during the hydrogen absorption hemicycle. Polarization time was 1 h. 0.5 M H<sub>2</sub>SO<sub>4</sub>.